Sub-nanometer Atomic Layer Deposition for Spintronics in Magnetic Tunnel Junctions Based on Graphene Spin-Filtering Membranes

Marie-Blandine Martin,[†] Bruno Dlubak,[†,‡] Robert S. Weatherup,[‡] Heejun Yang,[†,§,∥] Cyrile Deranlot,[†] Karim Bouzehouane,[†] Frédéric Petroff,[†] Abdelmadjid Anane,[†] Stephan Hofmann,[‡] John Robertson,[‡] Albert Fert,[†] and Pierre Seneor[†,*]

[†]Unité Mixte de Physique CNRS/Thales, 91767 Palaiseau, France and University of Paris-Sud, 91405 Orsay, France, [‡]Department of Engineering, University of Cambridge, Cambridge CB21PZ, United Kingdom, [§]IBS Center for Integrated Nanostructure Physics (CINAP), Institute of Basic Science, Sungkyunkwan University, Suwon 440-746, South Korea, and [∥]Department of Energy Science, Sungkyunkwan University, Suwon 440-746, South Korea

ABSTRACT We report on the successful integration of low-cost, conformal, and versatile atomic layer deposited (ALD) dielectric in Ni−Al_2O_3−Co magnetic tunnel junctions (MTJs) where the Ni is coated with a spin-filtering graphene membrane. The ALD tunnel barriers, as thin as 0.6 nm, are grown layer-by-layer in a simple, low-vacuum, ozone-based process, which yields high-quality electron-transport barriers as revealed by tunneling characterization. Even under these relaxed conditions, including air exposure of the interfaces, a significant tunnel magnetoresistance is measured highlighting the robustness of the process. The spin-filtering effect of graphene is enhanced, leading to an almost fully inversed spin polarization for the Ni electrode of −42%. This unlocks the potential of ALD for spintronics with conformal, layer-by-layer control of tunnel barriers in magnetic tunnel junctions toward low-cost fabrication and down-scaling of tunnel resistances.

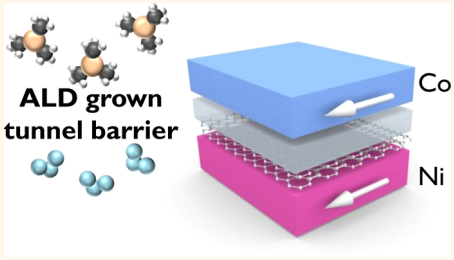

KEYWORDS: atomic layer deposition · spintronics · spin filter · graphene · dielectrics · magnetic tunnel junction

Atomic layer deposition (ALD) is a key technology for applications requiring ultrathin, uniform, high-quality, and conformal films. Owing to the chemically surface-limited growth mechanisms involved, ALD enables atomic control of the film thickness even for high aspect ratio substrates while being scalable and compatible with other industrial techniques such as roll-to-roll processing.[1−3] These advantages are already exploited in a number of applications, including multilayer stacks in thin film electroluminescent flat panel displays,[4,5] high-quality dielectrics in dynamic random access memory (DRAM) capacitors,[6,7] conformal passivation coatings for organic electronics, *e.g.*, organic light-emitting diodes (OLED),[8,9] and conformal functionalization for porous biomaterials and bioelectronic devices.[10,11] Furthermore, ALD-grown ultrathin, high-k gate dielectrics were industrially adopted for complementary metal oxide semiconductor (CMOS) logic technologies for high-volume manufacturing as early as the 45 nm node,[12] and ALD is particularly well adapted for the high aspect ratio architectures such as FinFET and TriGate transistors used in the current 22 nm node.[13,14]

To date, despite a number of pioneering attempts[15−19] with promising results, the advantages of ALD have not been widely employed in the field of magnetic tunnel junctions for spintronics, which has instead had to rely on more complex physical deposition setups. Spin valves, the active elements in technologies such as hard-drive read-heads and magnetic random-access memories (MRAM),[20] would appear to be prime candidates to benefit from the use of ALD:[15−17] spin devices rely heavily on ultrathin films such as nanometer-scale oxide tunnel barriers, whose quality and atomic composition crucially impact the electron's spin polarization. A key issue has however remained: performing ALD directly

* Address correspondence to pierre.seneor@thalesgroup.com.

Received for review March 20, 2014 and accepted July 2, 2014.

Published online July 02, 2014
10.1021/nn5017549

on metallic spin sources (usually ferromagnets such as Ni, Co, Fe, and their alloys) leads to their oxidation during the fabrication and thus a quenching of their spintronic performances. This has drastically limited the range of processes that can be used to fabricate spin-valve devices. Hence, although promising in terms of thickness and composition control, the application of water- or ozone-based ALD processes to magnetic tunnel junctions has so far been hindered by the associated ferromagnet oxidation.[15−17]

Here we demonstrate the successful realization of graphene-coated Ni/Al_2O_3/Co magnetic tunnel junctions based on sub-nanometer, ozone-based ALD-grown tunnel barriers. We are thus able to take advantage of the layer-by-layer thickness control, inherent to ALD, to down-scale the thickness and the resistance × area product of tunnel barriers. Measurements of large inverse tunnel magneto-resistance (TMR) signals highlight the almost full reversal of the graphene-coated Ni spin polarization ($P = -42\%$) compared to the max reported value ($P = +46\%$ for the highest quality Ni/Al_2O_3 interfaces[21]) and demonstrate the quality of the ALD barrier.

RESULTS AND DISCUSSION

In Figures 1 and 2, we present the technological steps employed to integrate ALD-grown tunnel barriers in vertical spin valves. Ni bottom electrodes are defined by a standard lift-off step, and a subsequent chemical vapor deposition (CVD) process[22,23] covers these electrodes with a continuous, few-layer graphene coating. This yields a reduced and passivated Ni surface.[24] This direct graphene growth method on patterned ferromagnetic electrodes is readily scalable and avoids graphene transfer or exfoliation steps otherwise typical for the fabrication of graphene devices.[25,26] A 1 μm^2 junction is then defined in the patterned resist (see Figure 1). Next, after exposing the bottom electrode to air, ALD is performed with cycles of ozone and trimethylaluminum (TMA) pulses to grow ultrathin Al_2O_3 layers (see Methods). This fabrication flow results in electrodes fully covered with an Al_2O_3 thin film. We note that the growth of ultrathin dielectrics on sp^2-bonded graphene coatings has previously been considered challenging:[27,28] both the preservation of the pristine graphene's sp^2 structure and the homogeneous wetting of the dielectric require careful engineering, which has been particularly discussed for films deposited by evaporation or water-based ALD. In particular, ALD on graphene has been shown to require surface seeding (such as modified ALD cycles, inorganic clusters, or molecular layers such as PTCA) to increase wetting as required for ultralow film thicknesses.[27−29] Interestingly, the unseeded ozone-based ALD (O_3-ALD) process used here is shown to be nondetrimental to the graphene layer (see Figure 3), while yielding Al_2O_3 films homogeneous enough to be used as tunnel barriers (see Figures 4 and 5).

As ozone is a powerful oxidant, its use in the process might be expected to result in significant oxidation of the graphene coating. We have thus investigated the impact of the whole O_3-ALD growth process on CVD graphene monolayers using Raman spectroscopy, for three different growth temperatures (T_{ch}): 80, 150, and 200 °C (see Figure 3). At the highest growth temperature of 200 °C, a strong Raman defect-enabled D peak (1350 cm^{-1}) appears in the spectra, with an amplitude even exceeding that of the graphitic G peak (1600 cm^{-1}), indicating a heavily degraded sp^2

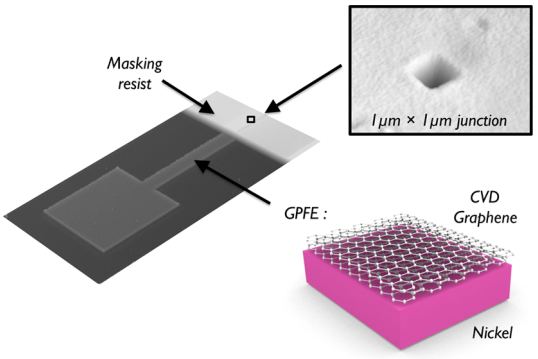

Figure 1. Optical profilometer image of a device. Junctions (1 μm^2) are opened in a masking resist on graphene-coated Ni electrodes derived by a direct CVD step.

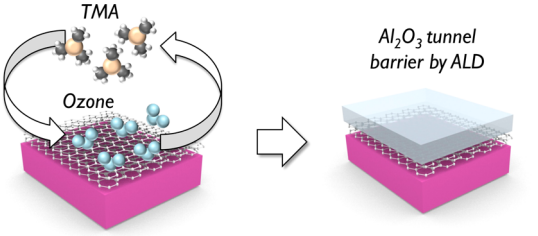

Figure 2. Schematic of the ozone-based atomic layer deposition process on graphene-coated electrodes. Ozone and trimethylaluminum (TMA) pulses are supplied, resulting in an electron-transparent Al_2O_3 tunnel barrier.

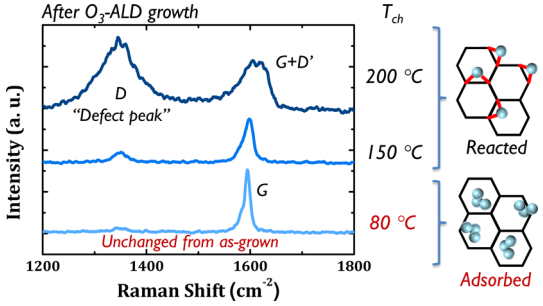

Figure 3. Raman spectra of CVD monolayer graphene on SiO_2 obtained after the growth of 1 nm Al_2O_3 by different ozone-ALD processes. In the case of the 80 °C process the Raman spectrum remains unchanged from as-grown graphene, indicating the preservation of the structural order of the graphene sp^2 lattice.

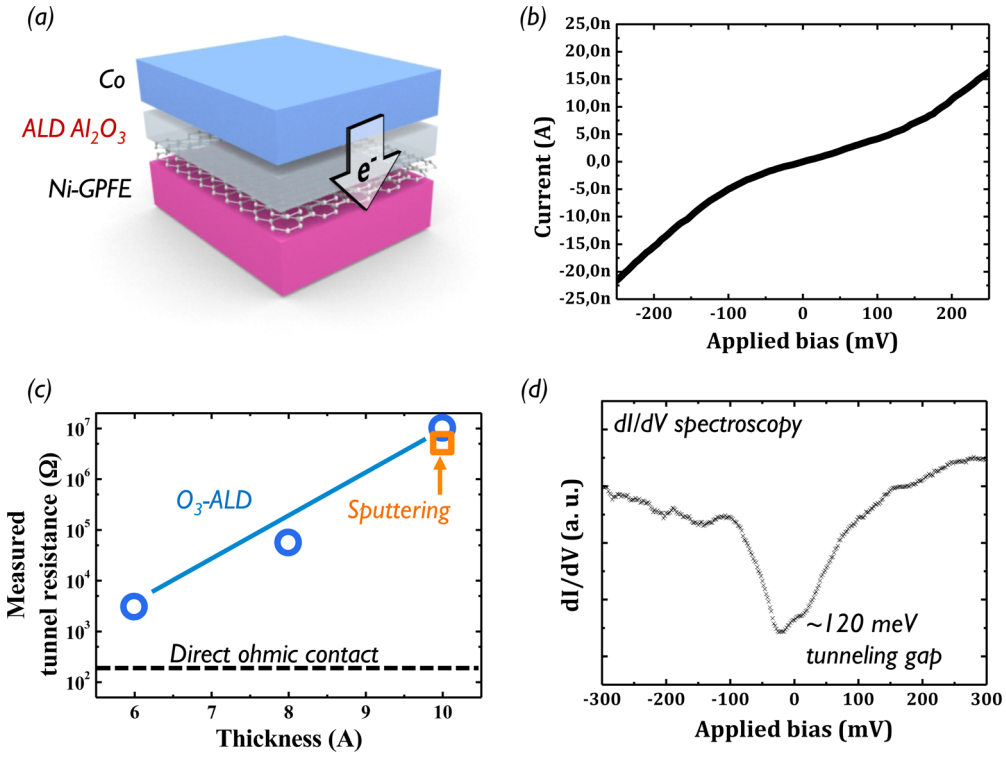

Figure 4. Electrical characterizations of ALD-grown tunnel barriers on graphene-coated electrodes obtained at 1.4 K. (a) Scheme of the graphene-coated Ni/ALD Al_2O_3/Co tunnel junction. (b) *I*−*V* curve measured for a 1 nm tunnel barrier with Resistance × Area product of about 20 Mohm·μm^2, (c) Exponential dependence of the resistance with the ALD barrier thickness as compared to 1 nm sputtered tunnel barriers. (d) d*I*/d*V* curve showing the typical gap-like feature arising from electron tunneling into graphene through ALD Al_2O_3.

structure.[30] Clearly at this high temperature, ozone reacts with the graphene layer introducing defects and forming functional groups such as epoxides on carbon sites.[31,32] Remarkably, however, this reactivity decreases sharply with lower growth temperature. In particular, Raman spectra measured after the 80 °C growth of Al_2O_3 remain unchanged compared to those measured on bare as-grown CVD graphene (see Figure 3): graphene appears to be inert to ozone during the 80 °C ALD process. These observations relate to the fact that ozone physisorption occurs on the graphene surface, while further chemical bonding between the oxygen and carbon atoms requires a non-negligible activation energy barrier to be overcome.[31,32] In the case of our 80 °C O_3-ALD process, the kinetics of this reaction are quenched for the exposure times considered. This inert process is thus considered in the following to grow ultrathin Al_2O_3 films in complete magnetic tunnel junctions.

Given the low wettability of the carbon sp^2 structure, another challenge is the formation of continuous, ultrathin, pinhole-free tunnel barriers on graphene. Despite it so far not being achievable by evaporation,[33] we previously reported that sputtering led to high-quality Al_2O_3 films on graphene down to a thickness of 1 nm.[34] However, growing Al_2O_3 films thinner than 1 nm on graphene by sputtering did not yield continuous layers. In particular, AFM characterization of a 0.6 nm tunnel barrier, produced by sputtering a 0.4 nm film of metallic Al that was further oxidized in a 50 Torr O_2 atmosphere (as for the high-quality 1 nm tunnel barrier[34]), reveals a particularly high roughness (RMS > 0.7 nm, even in excess of the targeted nominal film thickness). In fact, at these lower thicknesses the coalescence of Al islands is not achieved following the sputtering process, leading to severely pinholed films. In stark contrast, 0.6 nm of Al_2O_3 obtained by the O_3-ALD process on graphene shows significantly higher homogeneity and no observable pinholes, as confirmed by AFM. The measured root-mean-square (RMS) roughness of 0.25 nm for the 0.6 nm ALD film is comparable to what is achieved for the thicker, high-quality, 1 nm, sputtered films. These characteristics underline that the inherent attributes of ALD are well suited for the needs of spintronics devices in terms of producing conformal, ultrathin, high-quality, films. Indeed, in the following the <1 nm films grown by ALD are shown to be homogeneous enough to act as quality tunnel barriers.

These ultrathin electron-transparent tunnel barriers grown by O_3-ALD are then integrated into 1 μm^2 vertical graphene-coated Ni/Al_2O_3/Co magnetic tunnel junctions. The tunnel junctions are contacted by a Au-capped ferromagnetic Co top electrode to probe their charge and spin transport properties (as shown schematically in Figure 4a). We first consider their

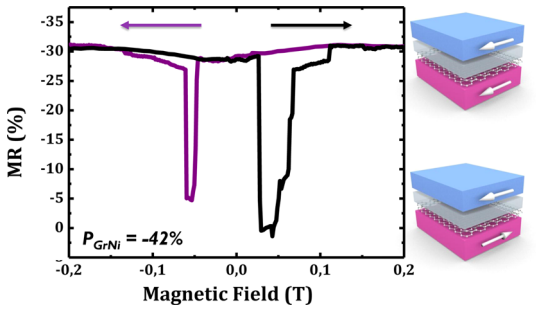

Figure 5. Large magneto-resistance signal obtained in graphene-coated Ni/ALD Al_2O_3/Co junctions. The inversed sign of the magneto-resistance arises from the negative spin polarization of the bottom electrode driven by the Ni/graphene interface spin-filtering effect.

electron tunneling properties. In Figure 4b, a typical $I-V$ transport characterization of a full tunneling spin valve is shown. We observe a strong nonlinear behavior. Next, in Figure 4c, the measured resistances of devices for the three different Al_2O_3 thicknesses are presented. Here, we note in particular that the 1 nm ALD tunnel barriers have resistances in the mega-ohm range, equivalent to results obtained with sputtered tunnel barriers.[24] The reduction of the number of ALD growth cycles allows the probing of electrical properties of thinner Al_2O_3 films (see Figure 4c): strikingly, the resistances measured for 0.6, 0.8, and 1 nm barriers scale exponentially with their thickness and show an increase by a factor 2 to 5 from 300 K down to 1.4 K. By comparison, junctions fabricated with a low-temperature water-based ALD process[28] systematically showed short-circuit characteristics with much lower resistances. Figure 4d shows a typical d*I*/d*V* spectrum measured at 1.4 K in these junctions. This spectrum contains a ~120 meV gap-like feature, which is characteristic of electron tunneling into graphene layers: at low biases, vertical tunneling is quenched due to the momentum mismatch between the tunneling electron and the available in-plane electron states in graphene, while at higher biases additional inelastic tunneling paths are activated.[35] These different electrical characterizations highlight the high quality of the Al_2O_3 layers grown by O_3-ALD as tunnel barriers.[36] Thus, the simple and low-cost O_3-ALD process presented here remarkably leads to well-wetted tunnel barriers on the bottom electrode with control down to extremely low thicknesses of 0.6 nm, below what is usually achievable by more sophisticated sputtering processes.[37,38]

We now discuss the spin transport properties of these tunnel devices. In Figure 5, a magneto-transport characterization obtained at 1.4 K is presented. Independent switching of the magnetizations of the top and bottom ferromagnetic electrodes allows the observation of two resistance states, revealing spin-dependent tunneling across the ALD layer. The large magneto-resistance (MR) measured confirms that the graphene passivation layer preserves a spin polarization for the bottom electrode following the ALD step. In contrast to unsuccessful previous studies where ALD was performed directly on top of ferromagnetic metals,[15−17] here we show that the graphene layer prevents the ferromagnet from oxidizing while allowing a spin-polarized current to be extracted. We obtain up to $MR = (R_{ap} - R_p)/R_{ap} = -31\%$ from the device characterization presented in Figure 5, where R_p and R_{ap} are the device resistances in the parallel and antiparallel state, respectively. The MR can be analyzed to extract the spin polarization P_{top} and P_{bot} of the top and bottom interfaces with $MR = 2P_{bot}P_{top}/(1 + P_{bot}P_{top})$, following ref 39. Taking the largest value of the Co/Al_2O_3 spin polarization we measure in reference devices[40] ($P_{top} = +32\%$), we derive a large $P_{bot} = -42\%$ for the air-exposed graphene-coated nickel/alumina. This negative sign was expected to arise from the nickel/graphene interface.[24,41] Strikingly, this is comparable in amplitude to the maximum reported $P = +46\%$ value difficultly achieved for the highest quality Ni/Al_2O_3 interfaces.[21] Hence this corresponds to a practically full inversion of the spin polarization *vs* graphene-free Ni/Al_2O_3 spin sources. The ability to achieve high spin signal amplitude from a Ni/Al_2O_3 source is remarkable when considering how difficult it has been to raise its spin polarization above +10% in state of the art tunneling experiments[21,42−44] and that the surface here has been exposed to air in this simple *ex situ* process. We note that the precleaning inherent to the O_3-ALD process used is able to remove contaminants from the air-exposed electrode. Another possible origin of this large MR signal could be the homogeneity of the Al_2O_3 layers grown by ALD. Indeed, high-quality sputtered Al_2O_3 tunnel barriers are usually produced by oxidizing a thin metallic Al film. This results in a gradient in the extent of oxidation through the layer while tunnel barriers grown by ALD are oxidized layer by layer, providing a more homogeneous material.[1,2] Following from the work presented herein, the layer-by-layer ALD growth of other tunnel barriers such as MgO can be foreseen. This may ultimately lead to higher spin polarization and drastically reduced resistances.

CONCLUSION

The ability to produce conformal, high-quality dielectrics in a layer-by-layer manner, combined with its notable simplicity and low cost, has led ALD to supersede other deposition techniques in many advanced microelectronics applications. Still, despite several attempts, its use has not been widely adopted for magnetic tunnel junctions where an industry-compatible alternative to sputtering has remained elusive. By demonstrating the fabrication of functional spin valves based on ultrathin and efficient ALD tunnel barriers, we unveil here the potential of ALD for spintronics and more particularly magnetic tunnel junctions. While this

is only the first step, ALD has a high potential and may open new avenues for the development of scaled-up spin circuits, such as MRAMs[45] and envisioned all-spin logic architectures,[46,47] offering closer integration with conventional processes of the microelectronics industry.

METHODS

Ni electrodes, 10 μm wide, are defined by e-beam lithography, evaporation of 150 nm of Ni, and subsequent lift-off. Reduction and graphene passivation of the Ni surface are achieved by a CVD process[22−24] performed in a custom-built cold-wall reactor whose base pressure is 5×10^{-7} mbar. Samples are heated in a 1 mbar atmosphere of H_2 to 600 °C at 300 °C/min and annealed for 15 min. The H_2 is removed, and then the samples are exposed to a 10^{-5} mbar atmosphere of C_2H_2 at 600 °C for 15 min. Finally, the samples are cooled in a vacuum at ∼100 °C/min. This growth results in a few-layer graphene (2−5 layers) coating, which prevents the oxidation of the Ni surface as checked by *in* and *ex situ* XPS measurements.[24] Complete spin valves are then fabricated using ALD tunnel barriers. Windows of 1 μm^2 are opened in a UVIII resist layer above the electrode by a second e-beam lithography step. Al_2O_3 layers of different thicknesses (0.6, 0.8, 1 nm) are grown by ALD using a Cambridge Nanotech Savannah system. The junctions are then contacted by a Co(15 nm)/Au(80 nm) top electrode sputtered through a shadow mask to protect bonding pads.

ALD is performed with the growth chamber temperature (T_{ch}) held at 80 °C, low enough to promote adsorption and quench ozone reactivity with graphene, yet high enough to enable complete ALD reactions. Ozone (500 Torr, 20 s purges) and trimethylaluminum (1 Torr, 60 s purges) pulses are sequentially carried out with a growth rate of 1 A per cycle. Before the growth, the graphene layers are exposed to a 500 Torr ozone atmosphere for 60 s to promote adsorption and subsequent homogeneous nucleation. CVD-like reactions in the chamber during the ALD process are prevented as checked by ellipsometry and breakdown measurements in mm^2 test structures. The quenching of the reactivity of the complete 80 °C ozone process with the graphene coating is probed by Raman spectroscopy with a Renishaw InVia system using a 532 nm laser. The roughness of the sputtered and ALD-grown tunnel barriers on graphene is characterized using AFM in tapping mode.

Conflict of Interest: The authors declare no competing financial interest.

Acknowledgment. R.S.W. acknowledges a Research Fellowship from St. John's College, Cambridge. P.S. acknowledges the Institut Universitaire de France for a junior fellowship. S.H. acknowledges funding from ERC Grant InsituNANO (No. 279342) and the EPSRC under Grant GRAPHTED (ref EP/K016636/1). This research was partially supported by the EU FP7 Work Programme under Grant GRAFOL (No. 285275) and Graphene Flagship (No. 604391).

REFERENCES AND NOTES

1. Leskelä, M.; Ritala, M. Atomic Layer Deposition Chemistry: Recent Developments and Future Challenges. *Angew. Chem., Int. Ed.* **2003**, *42*, 5548–5554.
2. Puurunen, R. L. Surface Chemistry of Atomic Layer Deposition: A Case Study for the Trimethylaluminum/Water Process. *J. Appl. Phys.* **2005**, *97*, 121301.
3. Kessels, W. M. M.; Putkonen, M. Advanced Process Technologies: Plasma, Direct Write, Atmospheric Pressure, and Roll-to-Roll ALD. *MRS Bull.* **2011**, *36*, 907–913.
4. Tiitta, M.; Niinistö, L. Volatile Metal Beta-Diketonates - ALE and CVD Precursors for Electroluminescent Device Thin Films. *Chem. Vap. Deposition* **1997**, *3*, 167–182.
5. Knez, M.; Nielsch, K.; Niinistö, L. Synthesis and Surface Engineering of Complex Nanostructures by Atomic Layer Deposition. *Adv. Mater.* **2007**, *19*, 3425–3438.
6. Kim, S. K.; Choi, G.-J.; Lee, S. Y.; Seo, M.; Lee, S. W.; Han, J. H.; Han, S.; Hwang, C. S. Al-Doped TiO_2 Films with Ultralow Leakage Currents for Next Generation DRAM Capacitors. *Adv. Mater.* **2008**, *20*, 1429–1435.
7. Niinistö, J.; Kukli, K.; Heikkilä, M.; Ritala, M.; Leskelä, M. Atomic Layer Deposition of High-k Oxides of the Group 4 Metals for Memory Applications. *Adv. Eng. Mater.* **2009**, *11*, 223–234.
8. Ghosh, A. P.; Gerenser, L. J.; Jarman, C. M.; Fornalik, J. E. Thin-Film Encapsulation of Organic Light-Emitting Devices. *Appl. Phys. Lett.* **2005**, *86*, 223503.
9. Keuning, W.; van de Weijer, P.; Lifka, H.; Kessels, W. M. M.; Creatore, M. Cathode Encapsulation of Organic Light Emitting Diodes by Atomic Layer Deposited Al_2O_3 Films and Al_2O_3/a-SiNx:H Stacks. *J. Vac. Sci. Technol. A* **2012**, *30*, 01A131.
10. Narayan, R. J.; Adiga, S. P.; Pellin, M. J.; Curtiss, L. A.; Hryn, A. J.; Stafslien, S.; Chisholm, B.; Shih, C.-C.; Shih, C.-M.; Lin, S.-J.; *et al.* Atomic Layer Deposition-Based Functionalization of Materials for Medical and Environmental Health Applications. *Philos. Trans. R. Soc. A* **2010**, *368*, 2033–2064.
11. Skoog, S. A.; Elam, J. W.; Narayan, R. J. Atomic Layer Deposition: Medical and Biological Applications. *Int. Mater. Rev.* **2013**, *58*, 113–129.
12. Mistry, K.; Allen, C.; Auth, C.; Beattie, B.; Bergstrom, D.; Bost, M.; Brazier, M.; Buehler, M.; Cappellani, A.; Chau, R.; *et al.* A 45nm Logic Technology with High-k+Metal Gate Transistors, Strained Silicon, 9 Cu Interconnect Layers, 193nm Dry Patterning, and 100% Pb-Free Packaging. *IEEE Int. Electron Devices Meet.* **2007**, 247–250.
13. Kavalieros, J.; Doyle, B.; Datta, S.; Dewey, G.; Doczy, M.; Jin, B.; Lionberger, D.; Metz, M.; Rachmady, W.; Radosavljevic, M.; *et al.* Tri-Gate Transistor Architecture with High-k Gate Dielectrics, Metal Gates and Strain Engineering. *Symp.VLSI Technol. Dig. Technol. Pap.* **2006**, 50–51.
14. Chau, R.; Doyle, B.; Datta, S.; Kavalieros, J.; Zhang, K. Integrated Nanoelectronics for the Future. *Nat. Mater.* **2007**, *6*, 810–812.
15. Bubber, R.; Mao, M.; Schneider, T.; Hegde, H.; Sin, K.; Funada, S.; Shi, S. ALCVD AlOx Barrier Layers for Magnetic Tunnel Junction Applications. *IEEE Trans. Magn.* **2002**, *38*, 2724–2726.
16. Mao, M.; Bubber, R.; Schneider, T. ALD for Data Storage Applications. *ECS Trans.* **2006**, *1*, 37–47.
17. Mantovana, R.; Vangelista, S.; Kutrzeba-Kotowska, B.; Cocco, S.; Lamperti, A.; Tallarida, G.; Mameli, D.; Fanciulli, M. Synthesis of Magnetic Tunnel Junctions with Full *in Situ* Atomic Layer and Chemical Vapor Deposition Processes. *Thin Solid Films* **2012**, *520*, 4820–4822.
18. Mantovan, R.; Vangelista, S.; Kutrzeba-Kotowska, B.; Lamperti, A.; Manca, N.; Pellegrino, L.; Fanciulli, M. $Fe_{3-\delta}O_4$/MgO/Co Magnetic Tunnel Junctions Synthesized by Full *in-Situ* Atomic Layer and Chemical Vapour Deposition. *J. Phys. D: Appl. Phys.* **2014**, *47*, 102002–102005.
19. Liu, X.; Shi, J. Magnetic Tunnel Junctions with Al_2O_3 Tunnel Barriers Prepared by Atomic Layer Deposition. *Appl. Phys. Lett.* **2013**, *102*, 202401.
20. Chappert, C.; Fert, A.; Van Dau, F. N. The Emergence of Spin Electronics in Data Storage. *Nat. Mater.* **2007**, *6*, 813–823.
21. Kim, T. H.; Moodera, J. S. Large Spin Polarization in Epitaxial and Polycrystalline Ni Films. *Phys. Rev. B* **2004**, *69*, 020403.
22. Weatherup, R. S.; Bayer, B. C.; Blume, R.; Ducati, C.; Baehtz, C.; Schlögl, R.; Hofmann, S. *In-Situ* Characterization of Alloy Catalysts for Low Temperature Graphene Growth. *Nano Lett.* **2011**, *11*, 4154–4160.
23. Weatherup, R. S.; Dlubak, B.; Hofmann, S. Kinetic Control of Catalytic CVD for High-Quality Graphene at Low Temperatures. *ACS Nano* **2012**, *6*, 9996–10003.

24. Dlubak, B.; Martin, M.-B.; Weatherup, R. S.; Yang, H.; Deranlot, C.; Blume, R.; Schloegl, R.; Fert, A.; Anane, A.; Hofmann, S.; *et al*. Graphene-Passivated Nickel as an Oxidation-Resistant Electrode for Spintronics. *ACS Nano* **2012**, *6*, 10930.
25. Mohiuddin, T. M. G.; Hill, E.; Elias, D.; Zhukov, A.; Novoselov, K.; Geim, A. Graphene in Multilayered CPP Spin Valves. *IEEE Trans. Magn.* **2008**, *44*, 2624–2627.
26. Cobas, E.; Friedman, A. L.; van't Erve, O. M. J.; Robinson, J. T.; Jonker, B. T. Graphene as a Tunnel Barrier: Graphene-Based Magnetic Tunnel Junctions. *Nano Lett.* **2012**, *12*, 3000–3004.
27. Kim, S.; Nah, J.; Jo, I.; Shahrjerdi, D.; Colombo, L.; Yao, Z.; Tutuc, E.; Banerjee, S. K. Realization of a High Mobility Dual-Gated Graphene Field-Effect Transistor with Al_2O_3 Dielectric. *Appl. Phys. Lett.* **2009**, *94*, 062107.
28. Dlubak, B.; Kidambi, P. R.; Weatherup, R. S.; Hofmann, S.; Robertson, J. Substrate-Assisted Nucleation of Ultra-Thin Dielectric Layers on Graphene by Atomic Layer Deposition. *Appl. Phys. Lett.* **2012**, *100*, 173113.
29. Jandhyala, S.; Mordi, G.; Lee, B.; Lee, G.; Floresca, C.; Cha, P.-R.; Ahn, J.; Wallace, R. M.; Chabal, Y. J.; Kim, M. J.; *et al*. Atomic Layer Deposition of Dielectrics on Graphene Using Reversibly Physisorbed Ozone. *ACS Nano* **2012**, *6*, 2722–2730.
30. Ferrari, A. C.; Robertson, J. Interpretation of Raman Spectra of Disordered and Amorphous Carbon. *Phys. Rev. B* **2000**, *61*, 14095.
31. Lee, G.; Lee, B.; Kim, J.; Cho, K. Ozone Adsorption on Graphene: Ab Initio Study and Experimental Validation. *J. Phys. Chem. C* **2009**, *113*, 14225–14229.
32. Leconte, N.; Moser, J.; Ordejon, P.; Tao, H.; Lherbier, A.; Bachtold, A.; Alsina, F.; Sotomayor, C. M.; Charlier, J.-C.; Roche, S. Damaging Graphene with Ozone Treatment: A Chemically Tunable Metal-Insulator Transition. *ACS Nano* **2010**, *4*, 4033–4038.
33. Popinciuc, M.; Józsa, C.; Zomer, P. J.; Tombros, N.; Veligura, A.; Jonkman, H. T.; Van Wees, B. J. Electronic Spin Transport in Graphene Field-Effect Transistors. *Phys. Rev. B* **2009**, *80*, 214427.
34. Dlubak, B.; Martin, M.-B.; Deranlot, C.; Bouzehouane, K.; Fusil, S.; Mattana, R.; Petroff, F.; Anane, A.; Seneor, P.; Fert, A. Homogeneous Pinhole Free 1 nm Al_2O_3 Tunnel Barriers on Graphene. *Appl. Phys. Lett.* **2012**, *101*, 203104.
35. Zhang, Y.; Brar, V. W.; Wang, F.; Girit, C.; Yayon, Y.; Panlasigui, M.; Zettl, A.; Crommie, M. F. Giant Phonon-Induced Conductance in Scanning Tunnelling Spectroscopy of Gate-Tunable Graphene. *Nat. Phys.* **2008**, *4*, 627–630.
36. Åkerman, J. J.; Slaughter, J. M.; Dave, R. W.; Schuller, I. K. Tunneling Criteria for Magnetic-Insulator-Magnetic Structures. *Appl. Phys. Lett.* **2001**, *79*, 3104.
37. Zhu, J.-G.; Park, C. Magnetic Tunnel Junctions. *Mater. Today* **2006**, *9*, 36–45.
38. Yuasa, S.; Djayaprawira, D. D. Giant Tunnel Magnetoresistance in Magnetic Tunnel Junctions with a Crystalline MgO(001) Barrier. *J. Phys. D: Appl. Phys.* **2007**, *40*, 337–354.
39. De Teresa, J. M.; Barthélémy, A.; Fert, A.; Contour, J.-P.; Lyonnet, R.; Montaigne, F.; Seneor, P.; Vaurès, A. Inverse Tunnel Magnetoresistance in $Co/SrTiO_3/La_{0.7}Sr_{0.3}MnO_3$: New Ideas on Spin-Polarized Tunneling. *Phys. Rev. Lett.* **1999**, *82*, 4288.
40. Barraud, C.; Deranlot, C.; Seneor, P.; Mattana, R.; Dlubak, B.; Fusil, S.; Bouzehouane, K.; Deneuve, D.; Petroff, F.; Fert, A. Magnetoresistance in Magnetic Tunnel Junctions Grown on Flexible Organic Substrates. *Appl. Phys. Lett.* **2010**, *96*, 072502.
41. Karpan, V. M.; Giovannetti, G.; Khomyakov, P. A.; Talanana, M.; Starikov, A. A.; Zwierzycki, M.; Van Der Brink, J.; Brocks, G.; Kelly, P. J. Graphite and Graphene as Perfect Spin Filters. *Phys. Rev. Lett.* **2007**, *99*, 176602.
42. Suezawa, Y.; Takahashi, F.; Gond, Y. Spin-Polarized Electron Tunneling in $Ni/Al_2O_3/Co$ Junction and Large Magnetoresistance of Ni/Co Double Layers. *Jpn. J. Appl. Phys.* **1992**, *31*, 1415–1416.
43. Meservey, R.; Tedrow, P. M. Spin-Polarized Electron Tunneling. *Phys. Rep.* **1994**, *238*, 173.
44. Monsma, D. J.; Parkin, S. P. P. Spin Polarization of Tunneling Current from Ferromagnet/Al_2O_3 Interfaces Using Copper-Doped Aluminum Superconducting Films. *Appl. Phys. Lett.* **2000**, *77*, 720.
45. Khvalkovskiy, A. V.; Apalkov, D.; Watts, S.; Chepulskii, R.; Beach, R. S.; Ong, A.; Tang, X.; Driskill-Smith, A.; Butler, W. H.; Visscher, P. B.; *et al*. Basic Principles of STT-MRAM Cell Operation in Memory Arrays. *J. Phys. D: Appl. Phys.* **2013**, *46*, 074001.
46. Behin-Aein, B.; Datta, D.; Salahuddin, S.; Datta, S. Proposal for an All-Spin Logic Device with Built-In Memory. *Nat. Nanotechnol.* **2010**, *5*, 266–270.
47. Seneor, P.; Dlubak, B.; Martin, M.-B.; Anane, A.; Jaffres, H.; Fert, A. Spintronics with Graphene. *MRS Bull.* **2012**, *37*, 1245–1254.